

Chapter 3:

**Regulation of Neural Crest Network Genes by Stem
Cell Factor Bmi-1 During Early Chick Development**

Jane Khudyakov, Tatjana Sauka-Spengler, and Marianne Bronner-Fraser

INTRODUCTION

The neural crest is a developmentally transient multipotent cell population that emigrates from the dorsal neural tube during neurula stages, migrates extensively throughout the body, and generates a diverse array of differentiated cell derivatives in a variety of target destinations (Le Douarin and Kalcheim, 1999). Neural crest cells are initially specified during gastrulation at the junction of the forming neural plate and non-neural ectoderm, as evidenced by the ability of gastrula-stage explants from this region to generate migratory neural crest cells autonomously in culture (Basch et al., 2006). However, neural crest cells do not differentiate *in vivo* until several days later, suggesting that multipotency is maintained for a significant period of their early development. In fact, back-transplantations and clonogenic assays have demonstrated that some multipotent neural crest cells continue to persist in targets such as the peripheral nerve, dorsal root ganglia, gut, and hair follicle, well into stages when neural crest-derived tissues were thought to be fully and irreversibly differentiated (Morrison et al., 1999; Crane and Trainor, 2006; Sieber-Blum and Hu, 2008). In addition, neuroblastoma tumors in pediatric patients are often neural crest-derived, suggesting that this cell type has the capacity to proliferate expansively and maintain a multipotent state that contributes to oncogenesis (Hemmati et al., 2003; Ross and Spengler, 2007). In light of these studies, the neural crest has been considered a type of stem cell, although some disagreement still exists as to whether it is strictly “stem” or “progenitor,” since isolated neural crest populations often contain a combination of both multipotent and lineage-restricted cells (Crane and Trainor, 2006).

Characterizing molecular mechanisms and cues that specify neural crest cells, contribute to maintenance of their plasticity and proliferation, and instruct their lineage-specific fate restriction and differentiation have been subjects of much interest. A putative neural crest gene regulatory network has been proposed which suggests that distinct groups of signals regulate successive steps in neural crest formation (Meulemans and Bronner-Fraser, 2004). For instance, inductive signals are received during gastrulation in the form of diffusible growth factors that subdivide the ectoderm into neural plate and non-neural ectoderm, inducing a group of transcription factors at their junction that specify this region as the neural plate border. These neural plate border specifiers then induce a group of neural crest specifier genes in the dorsal neural folds during neurulation, which label these cells as pre-migratory neural crest (Aybar and Mayor, 2002; Gammill and Bronner-Fraser, 2003). In turn, the neural crest specifiers induce a group of effector genes that enable migratory behavior and differentiation into particular neural crest derivatives (Sauka-Spengler and Bronner-Fraser, 2008). However, we now know that these relationships are not linearly hierarchical. For instance, many neural crest specifiers are co-expressed with neural plate border specifier genes in the chick gastrula in similar spatiotemporal patterns (Khudyakov and Bronner-Fraser, 2009). Therefore, at a time when neural crest cells are thought to be receiving their first specification signals, they already express a combination of induction factors and specifiers of both neural plate border and neural crest fate. This observation suggests that instructive molecular cues are present very early in neural crest development and function in a manner that involves extensive regulatory interactions.

Despite the presence of multiple components of the NC-GRN in the neural plate border during early development, this region contains a heterogeneous and intermixed population of neural crest, placode, and dorsal neural tube precursors which are indistinguishable (Fernandez-Garre et al., 2002; Hong and Saint-Jeannet, 2007; Ezin et al., 2009). Even after neural tube closure, progenitors in the dorsal neural tube can contribute to both neural crest and neural tube derivatives, and it is not until the former undergo an epithelial-to-mesenchymal transition that they become bona fide neural crest cells (Bronner-Fraser and Fraser, 1988; Bronner-Fraser, 1998, 2002). Therefore, although a number of specification factors are expressed continuously throughout neural crest development, the progenitors receiving these signals remain uncommitted and multipotent for quite some time. We hypothesize that maintenance of the multipotent neural plate border progenitor and undifferentiated neural crest cell may require regulation of neural crest network genes by yet unknown repressive mechanism(s).

Global regulation of developmental genes mediated by the Polycomb Group (PcG) of epigenetic repressors has been proposed as one of the main mechanisms involved in maintenance of a stable stem cell state in mouse and human embryonic stem cells (ESC) (Boyer et al., 2006; Bracken et al., 2006; Lee et al., 2006). The Polycomb proteins were first identified in *Drosophila* over 30 years ago as repressors of homeotic genes, and have subsequently been shown to function in axial patterning in vertebrates in a similar manner (Lewis, 1978; van der Lugt et al., 1996). PcG first began to attract the attention of the stem cell community when several protein partners were found to repress negative regulators of the cell cycle, therefore promoting self-renewal and preventing

premature senescence of hematopoietic and neural stem cells (Jacobs et al., 1999a; Molofsky et al., 2003; Park et al., 2003). More recent studies have demonstrated that PcG proteins serve to maintain ESC in a pluripotent, undifferentiated state by repressing a vast number of transcription factors and signaling molecules involved in development and differentiation (Pietersen and van Lohuizen, 2008; Schwartz and Pirrotta, 2008).

The Polycomb Group consists of two large, separate, and sequentially acting protein complexes, each of which contains a set of core components necessary for repression, as well as a number of other interchangeable protein partners (see Fig. 1.2B, Chapter 1). The core components of Polycomb Repressive Complex 2 (PRC) include the methyltransferase Ezh, which catalyzes addition of three methyl groups to lysine 27 of histone H3 (H3K27me³), a canonical mark of epigenetic repression. Chromodomain-containing protein partners of Polycomb Repressive Complex 1 (PRC1) subsequently recognize this methylation mark and the complex is recruited to the PRC2-associated target chromatin region (Schwartz and Pirrotta, 2007). The catalytically active PRC1 subunit Ring1B ubiquitinates histone H2A at lysine 119, which is thought to aid in stabilizing and maintaining PRC2-mediated repression (Wang et al., 2004; Cao et al., 2005).

While PcG binding sites or “Polycomb Repressive Elements” have been well characterized in *Drosophila*, analogous regions within vertebrate genomes have proven difficult to identify, although some correlations between CpG island distribution patterns and PcG binding have been made (Schwartz and Pirrotta, 2007; Ku et al., 2008). Recent whole-genome profiling studies of Polycomb binding by ChIP-on-Chip have demonstrated that core members of both complexes are associated with an impressive number of transcription factor

groups in stem cells and are often spread over chromatin regions several kilobases in size surrounding the coding regions of these genes (Bracken et al., 2006). As a general rule, PcG target genes, the majority of which represent key developmental regulators, remain transcriptionally silent until ESC are induced to differentiate, at which point the PcG is removed from chromatin and the genes are activated. Not surprisingly, ESC isolated from knockout mice lacking core PRC components differentiate prematurely in culture by inappropriately upregulating Polycomb target genes (Boyer et al., 2006; Lee et al., 2006).

Interestingly, PcG-associated chromatin regions are often marked not only by the repressive methylation mark H3K27me³ but also by trimethylated lysine 4 (H3K4me³), a mark of active transcription. These regions have been termed “bivalent” and are associated with genes that are “poised” to undergo a change in transcriptional activity upon differentiation (Bernstein et al., 2006; Ku et al., 2008). It therefore appears that the role of PcG in stem cell development is highly complex and involves maintenance of key developmental regulator genes in a transcriptionally plastic state that can be changed quickly upon reception of instructive signals. Moreover, Polycomb proteins are also necessary for proper cell differentiation because they repress “pluripotency” genes and regulators of alternative cell type pathways during lineage restriction (Pasini et al., 2007; Mohn et al., 2008). Therefore, the PcG proteins are critical regulators of embryonic development that fulfill a number of diverse functions, including (but probably not limited to) cell proliferation, maintenance of pluripotency, cell lineage restriction and differentiation, and axial patterning. Not surprisingly therefore, the Polycomb genes have been highly conserved throughout metazoan evolution (Whitcomb et al., 2007).

Due to the many similarities between ESC and neural crest progenitors, we hypothesized that Polycomb proteins may function analogously during neural crest development by repressing members of the NC-GRN. We chose to focus on PRC1 member Bmi-1 which has a well-studied role in proliferation and self-renewal of neural and hematopoietic stem cells (Park et al., 2004). Although it does not possess any enzymatic activity on its own, Bmi-1 has been shown to stimulate the ubiquitination activity of Ring1B and to maintain integrity of the PRC1 complex, possibly by acting as a tethering protein (Wang et al., 2004; Cao et al., 2005). In addition, ChIP studies have demonstrated that Bmi-1 associates with developmental regulator genes in embryonic stem cells, similarly to other PcG components (Bracken et al., 2006; Dietrich et al., 2007).

Chick *Bmi-1* was previously identified in a macroarray library screen and shown to be present throughout early chick development in a number of tissues, including the neural crest (Fraser and Sauka-Spengler, 2004). In this work, we demonstrate that *Bmi-1*, along with six other PcG genes, is expressed by neural crest progenitors from gastrulation until migration stages. Bmi-1 knock-down by *in vivo* antisense morpholino oligonucleotide electroporation results in an early upregulation of several neural crest network genes of the neural plate border and neural crest specifier categories in the absence of significant changes in cell proliferation within the dorsal neural fold. In contrast, combined over-expression of Bmi-1 and Ring1B in the early embryo results in a downregulation of the neural plate border specifier *Msx1*. Our results suggest that Bmi-1, as part of the PRC1 complex, negatively regulates expression of neural crest network genes during early chick development, possibly as a means of preventing premature

differentiation or modulating appropriate lineage restriction and cell fate decisions.

MATERIALS AND METHODS

Chick embryo incubation

Fertilized chicken eggs were obtained from AA Enterprises (Ramona, CA) and incubated at 38°C in a humidified incubator (Lyon Electric, Chula Vista, CA). Embryos were staged according to the Hamburger and Hamilton chick staging system (Hamburger and Hamilton, 1992).

***In situ* hybridization**

Chick embryos were dissected in Ringer's solution and fixed in 4% paraformaldehyde at 4°C overnight. Whole-mount *in situ* hybridization was performed as described previously (Nieto et al., 1996; Xu and Wilkinson, 1998), with some modifications involving more extensive washing adapted from a lamprey *in situ* protocol (Sauka-Spengler et al., 2007). Stained embryos were photographed in 50% glycerol on a Zeiss Stemi SV11 microscope using AxioVision software (Release 4.6) and processed using Photoshop 7.0 (Adobe Systems).

***In situ* mRNA probes**

The following DNA templates were used for antisense mRNA probe synthesis: cBmi-1 (Fraser and Sauka-Spengler, 2004), Pax7 (Basch et al., 2006), FoxD3 (Kos et al., 2001), Snail2 (Nieto et al., 1994), and Sox10 (McKeown et al., 2005). EST clones obtained from the BBSRC ChickEST Database (<http://www.chick.umist.ac.uk>) for use as *in situ* probe templates were the following: c-myc (ChEST191o11), Zic1 (ChEST459n6), AP-2 α (ChEST765g1), Irx1

(ChEST523e4), Msx1 (ChEST900p21), Ring1B (ChEST852k8), Phc1 (ChEST49d22, ChEST764m2), Cbx2 (ChEST992K16), Cbx8 (ChEST636k11), Eed (ChEST78C3), and Suz12 (ChEST848N23). The HoxA2 clone was obtained from Peter Lwigale. Linearized DNA was used to synthesize digoxigenin- and fluorescein-labeled antisense probes with Promega buffers and RNA polymerases (Promega Corporation). RNA probes were purified with illustra ProbeQuant™ G-50 Micro Columns (GE Healthcare, Cat# 28-9034-08).

Cryosectioning

To obtain transverse sections for histological analysis, embryos were equilibrated in 15% sucrose (in phosphate-buffered saline (PBS)) for 2 hours at room temperature, then transferred to 30% sucrose and incubated overnight at 4°C. Embryos were embedded in O.C.T. Compound (Tissue-Tek, catalog #4583) and frozen at -80°C. Sections 14 to 20 µm thick were obtained by cryosectioning at a temperature of -23°C on a Microm HM550 cryostat. For imaging without subsequent immunostaining, slides were washed twice for 10 minutes in PBS with 0.1% Tween, rinsed in double-distilled water, and mounted with PermaFluor Mountant Medium (Thermo Electron Corporation, Cat# 434990). Sections were imaged on a Zeiss Axioskop 2 Plus microscope and processed as described for whole-mount images.

Antibodies and immunohistochemistry

The distribution of Bmi-1 and Ring1B proteins was examined using the following antibodies: Anti-Bmi-1, clone F6 mouse monoclonal IgG1 (1:200, Upstate, Cat#

05-637), Rabbit polyclonal to Bmi-1 (1:500, Abcam, ab38432), and mouse monoclonal Ring1B (1:2000, Atsuta et al., 2001). Whole chick embryos were fixed in 4% paraformaldehyde at 4°C overnight, washed in PBS containing 0.1% Tween-20 (PBTw), and incubated in blocking solution (5% goat serum in PBTw) for 2 hours at room temperature. Primary antibody was added in blocking solution and incubated at 4°C overnight, then washed with PBTw, and replaced with Alexa-Fluor 488 or 568 secondary antibody (1:500 in PBTw, Molecular Probes) and incubated overnight at 4°C. Embryos were then washed, mounted, and imaged on a Zeiss Axioskop 2 Plus microscope and processed using Photoshop 7.0 (Adobe Systems). Alternatively, after the primary antibody step embryos were washed in 0.5% hydrogen peroxide in PBTw for 45 minutes, rinsed with PBTw, and incubated with biotin-labeled secondary antibody (1:750 in PBTw, Jackson Labs, Cat# 715-065-150, 711-065-152) overnight at 4°C. Following PBTw washes, embryos were incubated with 1:750 ABC reagent overnight at 4°C (Vectastain ABC kit, Vector Laboratories, Cat# PK-4000). After several PBTw washes, immunostaining was developed using 0.1 mg/mL DAB reagent in PBTw with 0.01% hydrogen peroxide and 0.001% NiCo (Sigma Fast 3.3 Diaminobenzidine Tablet Sets, Sigma, Cat# D-4293). Embryos were then washed with PBS containing 0.2% sodium azide, rinsed in PBTw, mounted, and imaged as described above. Fluorescent immunostaining on sections was performed using a similar protocol as described for whole-mount and the following primary antibodies: rabbit anti-phospho-histone H3 (1:2000, Upstate, Cat# 06-570), anti-HNK-1 (1:50, American Type Culture Collection Hybridoma), anti-GFP rabbit IgG fraction (1:500, Molecular Probes, Cat#A11122), anti-

HuC/HuD neuronal protein (human), mouse IgG_{2b} (1:500, Invitrogen, Cat#A-21271). Sections were incubated with 0.001% DAPI in PBTw for 5 minutes, rinsed with PBTw, and mounted with PermaFluor Mountant Medium (Thermo Electron Corporation, Cat# 434990). Sections were imaged on a Zeiss Axioskop 2 Plus microscope and processed as described for whole-mount images.

Morpholino design and specificity assay

3'-lissamine-labeled antisense cBmi-1 morpholino oligonucleotides were designed according to manufacturer's criteria (Gene Tools, LLC) as follows:

Bmi-1 MO1: 5'-TTTTGATCCTGGTCGTCCGGTGCAT-3', Bmi-1 MO2: 5'-GTCGTCCGGTGCATTTTGGCGCGGG-3'. The following 3'-lissamine-labeled 5

base pair mismatch cBmi-1 morpholinos were designed as negative controls:

Control MO1: TTTTcATCgTGGTgGTCCcGTcCAT-3', Control MO2: 5'GTCcTCCGcTGgATTTTGGaGCcGG-3' (mutated bases shown in lower case).

A 3' lissamine-labeled standard control MO (5'-CCTCTTACCTCAGTTACAATTTATA-3') provided by Gene Tools was also used

in control experiments. Morpholinos were dissolved in sterile water to a working concentration of 1 mM for chick embryo injection. A *Xenopus laevis* oocyte *in vitro*

translation system was used to evaluate MO specificity. Fertilized *Xenopus laevis*

embryos at the 1- to 2-cell stage were co-injected with 100 pg of *cBmi-1* mRNA containing a C-terminal myc tag and 10 ng of either Bmi-1, mismatch, or

standard control MO. Prior to injection, morpholinos and RNA were combined and incubated at 37°C for 30 minutes to confirm that RNA does not degrade in

these conditions. Injected *Xenopus* embryos were collected at gastrula stage and lysed in protein extraction buffer (50mM Tris, 100mM NaCl, 5mM EDTA and 1%

NP-40). Yolk was cleared from protein samples by extraction with an equal volume of Freon (1,1,2-Trichloro 1,2,2 trifluoroethane, Spectrum Laboratories Inc.) and resolved on a 12% SDS-PAGE gel. Anti-myc antibody was used for immunoblotting at 1:2000 concentration (9E10, Santa Cruz Biotechnology, Inc).

Electroporation

HH stage 3-5 chick embryos were explanted on Whatman filter paper rings and placed ventral-side up in Ringer's solution in an electroporation dish containing a platinum plate electrode on the bottom of a shallow well. Bmi-1 or control morpholinos at 1mM concentration were unilaterally injected into the lumen between the epiblast and vitelline membrane targeting the prospective neural plate border. The embryo was covered with a flattened-tip platinum electrode and five 7-volt, 50-millisecond pulses with 100 millisecond pauses in between were applied using a square-pulse electroporator. Embryos were cultured in thin albumin in a humidified 37°C incubator. After 6-24 hours, embryos were fixed in 4% paraformaldehyde for analysis by *in situ* hybridization and subsequently dehydrated to 100% methanol, or dissected and lysed in 100 µL of RNAqueous®-Micro Lysis Buffer (Ambion, Cat# AM1931) for RT-QPCR assay.

Over-expression constructs

Using a high fidelity enzyme (Expand High FidelityPLUS PCR System, Roche, Cat# 03300242001), the open reading frame including endogenous Kozak sequence was amplified using the full-length Bmi-1 clone obtained previously from a chick cDNA library screen as a template (Fraser and Sauka-Spengler,

2004). The resulting fragment was cloned into several expression vectors: pCIG-IRES-GRP (pCIG-Bmi-1-GFP), pCIG-H2B-GFP (pCIG-Bmi-1-H2B-GFP), and pCIG-H2B-RFP (pCIG-Bmi-1-H2B-RFP). Full-length Ring1B was obtained by screening a chick cDNA library using a Ring1B EST clone (ChEST852k8, BBSRC ChickEST Database <http://www.chick.umist.ac.uk>) (Gammill and Bronner-Fraser, 2002). Similarly, the Ring1B ORF with Kozak sequence was cloned into several expression vectors: pCIG-IRES-GRP (pCIG-Ring1B-GFP), pCIG-H2B-RFP (pCIG-Ring1B-H2B-RFP), and pCIG-mem-RFP (pCIG-Ring1B-memRFP (RFP with a membrane linker)). Maxi preps were prepared using the Qiagen EndoFree Plasmid Maxi Kit (Qiagen, Cat# 12362) and DNA was re-suspended in Buffer EB (Qiagen, Cat# 19086). Plasmids were further diluted to a concentration of 2 to 5 $\mu\text{g}/\mu\text{L}$ with Buffer EB and 0.01% Blue Vegetable Dye (FD&C Blue 1, Spectra Colors Corp, Cat# 3844-45-9) for injection into chick embryos as described for morpholinos. Empty vectors were used as electroporation controls.

RNA and cDNA preparation

Total RNA from electroporated embryos was isolated using the RNAqueous®-Micro Lysis Kit (Ambion, Cat# AM1931). Genomic DNA was digested using TURBO DNA-free™ (Ambion, Cat# AM1907) according to manufacturer's protocol with the exception of extended digestion time and increased quantity of enzyme. Clean total RNA was precipitated and concentrated and cDNA was synthesized using random hexamers and SuperScript® II Reverse Transcriptase (Invitrogen, Cat# 18064-022) according to the manufacturer's instructions.

QPCR

QPCR was performed using the 96-well plate ABI 7000 QPCR machine (Applied Biosciences) with SYBRGreen iTaq Supermix with ROX (Bio-Rad, Cat# 172-5101). Primers were used at 450 nM concentration in a 25 μ L reaction. Gene-specific primers were designed using the Primer 3 program (<http://frodo.wi.mit.edu>) and synthesized by IDT. The sequences of primers used are as follows: Msx1 F 5'- GGAAGTGTGGCAGAGAAAGG-3', Msx1 R 5'- ATGGCCACAGGTTAACAGC-3', Pax7 F 5'-ACTGCGACAAGAAGGAGGAA-3', Pax7 R 5'-CTCTTCAAAGGCAGGTCTGG-3', FoxD3 F 5'-TCTGCGAGTTCATCAGCAAC-3', FoxD3 R 5'-TTCACGAAGCAGTCGTTGAG-3', Sox9 F 5'-CTCAAGGGCTACGACTGGAC-3', Sox9 R 5'-CTTCACGTGGGGTTTGTCT-3', Gapdh F 5'-GGACACTTCAAGGGCACTGT-3', Gapdh R 5'-TCTCCATGGTGGTGAAGACA-3'. Each sample was run in three replicates to reduce errors created by pipetting. The baseline and threshold levels were set according to the Applied Biosystem software, and gene expression was calculated by the standard curve assay method as described in the Applied Biosystems protocols. In detail, the results for different samples were interpolated from a line created by running four point standard curves for each primer set and then normalized against results for the *Gapdh* housekeeping gene. The standard cDNA was prepared from chick embryos collected during stages when all the target genes are known to be expressed in measurable quantities. Each plate also held two minus RT controls for each set of primers, which showed no amplification. Fold amplification was calculated as the ratio of

normalized expression levels between the electroporated and control sides of the same embryo.

RESULTS

***Bmi-1* is expressed in neural crest progenitors during gastrulation**

The expression pattern of chick *Bmi-1* during early development was characterized in detail by whole-mount *in situ* hybridization using a full-length antisense RNA probe (Fraser and Sauka-Spengler, 2004). During early gastrulation (Hamburger and Hamilton (HH) stage 3c, Hamburger and Hamilton, 1992), *Bmi-1* is expressed ubiquitously and at low levels throughout the epiblast (Fig. 3.1A). As gastrulation proceeds, *Bmi-1* transcripts begin to accumulate at the presumptive neural plate border, both posteriorly and anteriorly, and are also maintained at lower levels in the prospective neural plate (Fig. 3.1B and C). *Bmi-1* is restricted to the ectodermal cell layer at HH4 (Fig. 3.1C,C'). *Bmi-1* expression during gastrulation was compared to early expression domains of several neural plate border and neural crest specifier genes. *Bmi-1* is expressed in the neural plate border in a domain similar to that of *Pax7* at HH4+ (Fig. 3.1D). However, *Pax7* is specific to cells in the presumptive neural plate border whereas the expression domain of *Bmi-1* is wider, more closely resembling that of *N-myc* (Fig. 3.1E). *Bmi-1* expression is restricted to the neural plate and its border, similarly to *Zic1*, and does not extend into non-neural ectoderm (Fig. 3.1F).

Bmi-1 expression in the neural plate border at HH4 was further characterized by double *in situ* hybridization. We find that it is co-expressed in the posterior neural plate border with *Msx1* (Fig. 3.1G). Anteriorly, *Bmi-1* is co-expressed with the placodal marker *Irx1* (Fig. 3.1H). It is excluded from non-neural ectoderm marked by *Dlx5* and *Msx1* (Fig. 3.1G and I). Therefore, we find

that chick *Bmi-1* is expressed by progenitors of neural, neural plate border, and placode fates during gastrulation.

***Bmi-1* is maintained in undifferentiated neural crest progenitors**

Bmi-1 transcripts persist in neural crest and neural tube progenitors during neurulation and neural crest migration. *Bmi-1* is expressed in and around the neural plate border at HH5 (Fig. 3.2A). During HH6, when neural folds begin to thicken, *Bmi-1* is expressed throughout the neuroepithelium and is obvious at the neural plate border (Fig. 3.2B,B'). Expression is highest during HH7 and HH8 in the anterior-most neural folds marked by *Zic1*, *c-myc*, and *N-myc* that do not generate neural crest cells (Fig. 3.2C,D; also see Fig. 2.2, Chapter 2). *Bmi-1* transcripts accumulate in the dorsal portion of the neural folds at HH8 (Fig. 3.2D'). After neural tube closure, *Bmi-1* marks pre-migratory neural crest cells in its dorsal aspect, as well as migrating neural crest cells (Fig. 3.2E,F,F',F').

Bmi-1 protein can be detected as early as HH3 and is localized in essentially the same domain as mRNA at these stages, suggesting that *Bmi-1* is actively translated in neural crest progenitors during early development (Fig. 3.3A-F). *Bmi-1* transcript expression is maintained in migrating neural crest cells until they reach their target tissues and begin to express markers of differentiation. For instance, HuC/D-positive neural crest-derived neurons in cranial ganglia do not express *Bmi-1* (Fig. 3.2G,G',G'',H,I). However, *Bmi-1* persists in other regions of the embryo that are not populated by neural crest, such as brain neuroectoderm and dermamyotome, suggesting additional functions in development of other cell types (Fig 3.2G). In conclusion, transcript and protein expression data demonstrate that undifferentiated neural crest

progenitors are marked by *Bmi-1* until they populate their target tissues and commence a terminal differentiation programme.

Multiple members of PRC1 and PRC2 are expressed in neural crest progenitors in overlapping domains

Bmi-1 functions as part of a large two-part protein complex, in which the presence of a set of “core” PRC2 and PRC1 partners is necessary for functional repression of target genes (Schwartz and Pirrotta, 2007). Therefore, we hypothesized that a number of other PcG genes may be co-expressed with *Bmi-1* in neural crest progenitors. Indeed, we find that transcripts of four PRC1 genes (*Ring1B*, *Phc1*, *Cbx2*, *Cbx8*) and two PRC2 genes (*Eed*, *Suz12*) are expressed in overlapping, but not identical domains during early neural crest development. During gastrulation (HH4/4+), *Cbx2* and *Eed* are expressed ubiquitously throughout the epiblast (Fig. 3.4C,E). In contrast, *Ring1B*, *Cbx8*, and *Suz12* are localized more specifically in the anterior epiblast corresponding to the prospective neural plate (Fig. 3.4A,D,F). *Phc1* exhibits the most specific expression pattern in the neural plate border, which is strikingly similar to that of *N-myc* (Fig. 3.4B) (Khudyakov and Bronner-Fraser, 2009). During neurulation (HH6-7) all six genes examined are expressed in the neural folds. *Ring1B*, *Cbx2*, *Eed*, and *Suz12* are expressed in neural tissue at all axial levels (Fig. 3.4G,I,K,L), whereas *Phc1* and *Cbx8* are mainly restricted to the anterior neural folds (Fig. 3.4H,J). In addition, *Ring1B*, *Cbx2*, *Eed*, and *Suz12* are expressed in anterior non-neural and non-placogenic ectoderm, and *Phc1* is distributed widely throughout ectoderm and area opaca at all axial levels. Strikingly, at HH8, all six genes are strongly expressed similarly to *Bmi-1* in the anterior-most neural folds, which fail

to generate neural crest (Fig. 3.4M-R). Transcripts also overlap in the open neural plate and lateral plate mesoderm. *Phc1* is the sole member maintained in the area opaca (Fig. 3.4N). During HH10, we find that all of the PcG genes examined are expressed in migrating cranial neural crest cells, trunk neural tube, and open neural plate, as well as in mesodermal and ectodermal tissues (Fig. 3.4S-X). In summary, we find that a number of PRC1 and PRC2 genes are expressed by neural crest progenitors during early development. Although their expression domains are broad, we were surprised to find that they are not ubiquitous, as might be assumed for catalytically active PcG genes that are critical for embryonic development (such as *Ring1B*), and for members of the upstream PRC2 complex (Voncken et al., 2003; Pasini et al., 2004). Although *Phc1* is the only gene with unique and specific expression in the neural plate border, all of the PRC expression domains examined encompass this territory, and all are also co-expressed in migrating cranial neural crest cells around HH10.

Bmi-1 knock-down results in early upregulation of the neural crest network genes

Msx1 is specifically upregulated as a result of *Bmi-1* MO electroporation

To examine the role of *Bmi-1* in early development of neural crest, we used a morpholino oligonucleotide-based loss-of-function approach. We designed two morpholinos (MOs) targeting the ATG context of chick *Bmi-1* and find that, when co-injected with myc-tagged *Bmi-1* mRNA into *Xenopus* embryos, they inhibit *Bmi-1* protein translation (Fig. 3.5I). We used these two MOs interchangeably in our experiments. MO electroporation was performed at HH stage 4 to target the prospective neural plate border region in one half of the

chick gastrula. Electroporated embryos were cultured in albumin until HH6-8 and analyzed by *in situ* hybridization. We find that Bmi-1 knock-down results in a consistent increase of *Msx1* transcripts in dorsal neural tube progenitors, visualized as an increase in staining intensity within its endogenous expression domain on the electroporated side (Fig. 3.5A,A',B,B',C,D,G, n=12/18 embryos, $p < 0.01$), which is not seen with control MO (Fig. 3.5E,E',F,F',G, n=2/13 embryos). Phenotypes range in severity and include a slight enhancement of staining along the AP axis of the embryo (Fig. 3.5D, n=5/18), or a strong increase in staining intensity within the neural fold edge and/or at the open neural plate (Fig. 3.5B, n=7/18). The effect is more discernable when electroporated embryos are analyzed at younger stages, and is often strongest within the open neural plate, suggesting that Bmi-1 may have an early role in regulating *Msx1*, and/or that the neural crest population is able to compensate for the MO effect as development proceeds. Interestingly, although the MO was often distributed throughout the whole proximo-distal aspect of the neural fold and the laterally adjacent ectoderm, ectopic expression of *Msx1* was never observed outside of the neural plate border, suggesting that Bmi-1 may act on *Msx1* specifically within this cell population.

We analyzed the effect of Bmi-1 MO on expression of several other neural plate border and neural crest specifier genes. We were unable to detect a statistically significant change in expression of the neural plate border specifier *Pax7* (n=3/13 weak upregulation). Likewise, preliminary *in situ* hybridization analysis did not suggest an effect of Bmi-1 MO on *Zic1*, *c-myc*, or *AP-2* expression. It is likely that while we do not observe a visible change in expression of these genes on the electroporated side of the embryo due to their

wide expression domains (as compared with *Msx1*), the transcript levels may be quantitatively altered. Alternatively, Bmi-1 may be regulating some neural crest network genes selectively.

The effects of Bmi-1 MO on neural crest specifiers are non-specific during late neurulation

In contrast to the effect on *Msx-1*, results of Bmi-1 knockdown on neural crest specifier genes during late neurulation stages were inconsistent. For *Snail2* and *FoxD3* expression, some Bmi-1 MO-electroporated embryos showed either a distinct anterior expansion or an anterior loss or general decrease on the electroporated side when analyzed at HH stage 8+/9, but which was not statistically significant (*Snail2*: n=6/17 upregulation, n=5/17 downregulation; *FoxD3*: n=4/11 downregulation, data not shown). A small number of control MO-electroporated embryos also exhibited non-specific effects when assayed for *FoxD3* (n=2/9) and *Snail2* (n=2/7) expression (data not shown). The Bmi-1 MO effect is most likely not secondary to changes in axial patterning because preliminary data suggest that expression of *HoxA2* may be unaltered (data not shown), which we found surprising in light of the role of Bmi-1 in homeotic repression in other organisms, although effects on other antero-posterior (AP) patterning genes were not examined (Lewis, 1978; van der Lugt et al., 1996; Cao et al., 2005). We hypothesize that these aberrant changes in gene expression may be secondary to the effect of Bmi-1 knock-down on the upstream specifier *Msx1* and possibly other unknown repressors or activators, as well as due to extensive cross-regulation between the neural crest specifiers (Gammill and Bronner-Fraser, 2002; Meulemans and Bronner-Fraser, 2004; Raible, 2006).

However, a large proportion of Bmi-1 MO-electroporated embryos assayed at late neurulation stages displayed no obvious phenotype (n=6/11 *FoxD3*, n=6/17 *Slug*, data not shown). In addition, condensation of ganglia and cranial and trunk neural crest migration patterns did not appear visibly altered in electroporated embryos assayed for *Sox10* and HNK-1 expression at later stages of development (data not shown). Because the neural crest is highly plastic and self-regulating as a cell population, examining effects of gene perturbations at later stages of development can be difficult due to extensive compensation (Le Douarin, 2004; Raible, 2006). Therefore, we can conclude from our analysis that the neural plate border specifier *Msx1* is negatively regulated by Bmi-1 during early neural crest development. However, we are unable to assess by *in situ* hybridization the later effects of Bmi-1 knock-down on downstream specifier genes and later events in neural crest migration and differentiation due to the extensive cross-regulatory relationships between such genes and the highly plastic and compensatory nature of this cell population.

Msx1, FoxD3, and Sox9 transcripts are quantifiably increased by Bmi-1 knock-down at HH6

To quantify changes in transcript levels as a result of Bmi-1 knock-down, we used real-time quantitative RT-PCR. HH4 embryos were electroporated with either Bmi-1 MO or control MO and cultured until HH6-10. Embryos collected at specific stages were then laterally bisected to separate the electroporated and control sides, followed by extraction of total RNA and cDNA synthesis from each embryo half. Real-time quantitative PCR was performed to compare changes in expression levels of several neural crest network genes between the control and

electroporated halves within the same embryo. In agreement with the *in situ* hybridization data, there is a twofold increase in *Msx1* expression in Bmi-1 MO-electroporated embryos assayed at HH6 (Fig. 3.6A,E, n=5, p<0.01). The fold change in transcript levels due to Bmi-1 knock-down is reduced or unchanged in embryos analyzed at later stages, likely due either to compensation by the neural crest population or dilution of MO as cells proliferate (Fig. 3.6A).

Similarly to *in situ* hybridization results, there is no significant change in *Pax7* (Fig. 3.6B) or *Sox10* (data not shown) expression with Bmi-1 MO. Changes in *Snail-2* expression are inconsistent, similar to *in situ* results, perhaps due to complex cross-regulatory interactions between the two genes and other neural crest specifiers (data not shown; Meulemans and Bronner-Fraser, 2004; Bermejo-Rodriguez et al., 2006; Sakai et al., 2006). In contrast, there is a greater than twofold increase in *FoxD3* (Fig. 3.6C,F, n=5, p<0.05) and *Sox9* (Fig. 3.6D, n=4, p<0.01) expression, respectively, in Bmi-1 MO-electroporated embryos collected at stage HH6, an effect that is difficult to discern by *in situ* hybridization due to low expression levels at this stage. As with *Msx1*, we do not see a significant effect on *FoxD3* and *Sox9* expression when we assay electroporated embryos at later developmental time points (Fig. 3.6C,D). This observation suggests that Bmi-1 also negatively regulates the neural crest specifiers *FoxD3* and *Sox9*, perhaps by preventing their early induction, upregulation or recruitment to the dorsal neural folds. Thus, quantification of transcript levels by real-time PCR is extremely sensitive and allows for detection of gene expression changes during early stages at which they are difficult to detect by *in situ* hybridization, and before phenotypic compensation occurs.

Upregulation of neural crest genes due to Bmi-1 MO occurs in the absence of changes in cell proliferation in the dorsal neural folds

Next, we investigated whether upregulation of neural crest network genes caused by Bmi-1 MO is the result of an increase in cell proliferation. We found a 19% increase in the mean number of phospho-histone H3 (PH3)-positive cells on the Bmi-1 MO-electroporated as compared to the control side in sections of six embryos which showed obvious upregulation of *Msx1* by *in situ* (Fig 3.5H, n=6, p<0.05). However, the effect was most often observed in adjacent non-neural ectoderm or within the lumen of the neuroepithelium, as opposed to the *Msx1*-positive dorsal aspect of the neural fold (Fig. 3.5A',B'). In contrast, we did not find a significant change in the number of PH3-positive cells in sections of four control MO embryos (Fig. 3.5E',F',H). In addition, we did not observe a decrease in cell proliferation or an abundance of pyknotic nuclei on the Bmi-1 MO-electroporated side in three embryos which showed a drastic decrease of *FoxD3* at HH8-9 (data not shown).

Therefore, although Bmi-1 transgenic mice exhibit strong defects in proliferation and cell survival, we did not observe a similar effect on progenitor cells within the dorsal neural fold and dorsal neural tube of HH6-9 chick embryos with *in vivo* Bmi-1 knock-down (Molofsky et al., 2003; Park et al., 2003). This is likely due to low penetrance of electroporated MO knock-down as compared with the mouse knockout system, as well as the fact that neural crest progenitors do not proliferate extensively until they begin migration, a time during which Bmi-1 may be acting more specifically on their cell cycle. Consequently, we conclude that Bmi-1 may act to regulate early transcription of neural crest network genes independently of changes in the cell cycle, possibly

by restricting the number of cells within the heterogeneous neural plate border population that express these genes and that are recruited as dorsal neural tube progenitors.

Co-over-expression of Bmi-1 and Ring1B causes a decrease in *Msx1* expression

We next performed the reciprocal experiment whereby Bmi-1 was overexpressed in the embryo under the control of the constitutively active chick beta-actin promoter (pCIG) to determine whether a large increase in Bmi-1 protein may enhance its repressive effect on neural crest genes. Although we did not examine large numbers of embryos, no significant or consistent change in expression of *Msx1* (n=6), *FoxD3* (n=4), or *HoxA2* (n=4) was observed when pCIG-Bmi-1-GFP was overexpressed at HH4 and embryos were subsequently assayed at stages ranging from HH6 to HH11. In addition, preliminary results suggest that there is no effect on *Snail2* and *Sox10* expression levels by *in situ* hybridization (data not shown). In order to determine whether over-expression of Bmi-1 may affect neural crest migration or contribution to sensory ganglia, we electroporated pCIG-Bmi-1-GFP into the neural fold on one side of the embryo at HH8 and cultured the embryos until HH13-17. We found that GFP-positive cells emigrated normally from the dorsal neural tube, migrated along unaltered pathways, expressed *Sox10* and HNK-1, contributed to cranial and dorsal root ganglia, and did not exhibit a change in cell proliferation (data not shown). However, we were unable to assess whether neural crest differentiation within the ganglia was affected by Bmi-1 over-expression due to the difficulty of culturing embryos to older stages, dilution of the electroporated construct with

cell division, and the highly self-regulating nature of the neural crest cell population.

In addition to the obstacles described above, it is also unlikely that over-expression of one member of a large protein complex would exhibit a significant increase in the functionality of the complex and a consequent effect on neural crest development. In accordance with this, over-expression of Ring1B alone had no effect on *Msx1* expression (data not shown). Therefore, we decided to co-electroporate pCIG-Bmi-1-GFP together with pCIG-Ring1B-memRFP (RFP with a membrane linker) at high concentrations into the prospective neural plate border at HH4, which resulted in an overabundance of translated Bmi-1 and Ring1B proteins by HH6 (Fig. 3.7A,B). Embryos co-electroporated with Bmi-1 and Ring1B exhibited a statistically significant decrease in *Msx1* staining intensity at HH6-8 (Fig. 3.7C,D,E, n=9/18, p<0.05) that was not observed in embryos electroporated with the empty control vector (Fig. 3.7F,G,E, n=2/17). However, expression of *FoxD3*, *Snail2*, or *Sox10* was unaffected when assayed at later stages (data not shown). This suggests that Bmi-1 cooperates with Ring1B to negatively regulate *Msx1* during early neural crest development. However, the effects on other, later-acting neural crest network genes were difficult to discern. Over-expression of at least three PcG genes may be required to elicit a strong effect on expression of neural crest genes. In particular, the specific expression pattern of *Phc1* during early neural crest development makes it a promising candidate for perturbation studies in combination with Bmi-1 and Ring1B. In summary, the preliminary co-over-expression results strongly suggest that Bmi-1, as part of PRC1, plays a role in repressing *Msx1*.

DISCUSSION

We have found that seven members the Polycomb group of epigenetic repressors are expressed in the chick embryo during early development in large and overlapping, but non-ubiquitous domains. During gastrulation, the PRC1 members *Bmi-1* and *Phc1* exhibit a strikingly specific expression pattern in the neural plate border, a region of the epiblast that has been shown to contain neural crest progenitors by fate-mapping analysis and explant experiments (Basch et al., 2006; Ezin et al., 2009). The expression domains of *Bmi-1* and *Phc1* are highly similar to that of *N-myc*, which is interesting in light of work that has demonstrated that *myc* genes collaborate with *Bmi-1* in lymphomagenesis, a process that involves rapid proliferation of hematopoietic stem cells (Haupt et al., 1993; Jacobs et al., 1999b). We also found that *Ring1B*, *Cbx8*, *Suz12*, *Cbx2* and *Eed* transcripts are expressed in the epiblast during gastrulation, and although their domains are large, they include the presumptive neural plate border.

During neurulation, all PcG genes examined thus far are expressed in the neural folds, and some are additionally present in ectoderm. Intriguingly, we find that *Bmi-1* and other PcG genes are strongly expressed at HH8 in the anterior-most neural folds that contain forebrain and olfactory progenitors but do not generate neural crest. An intriguing possibility is that a Polycomb-mediated repressive mechanism restricts neural crest formation to the anterior boundary of the midbrain, consistent with the role of PcG genes in Hox boundary regulation and antero-posterior (AP) patterning (Alkema et al., 1995; van der Lugt et al., 1996; Le Douarin and Kalcheim, 1999; Cao et al., 2005). Accordingly, mouse knockouts of some PRC1 genes exhibit posterior

transformations and neural crest defects due to incorrect rhombomere and branchial arch patterning, although the phenotypes have not been examined at earlier stages of development (Takahara et al., 1997; Tomotsune et al., 2000).

We also find that all of the PcG genes that we examined thus far are expressed in migrating cranial neural crest at HH10, as well as in other tissues such as lateral non-placogenic ectoderm, lateral plate mesoderm, and blood. PRC expression in blood islands is not surprising since Polycomb genes are known regulators of hematopoietic stem cell development in other organisms (Lessard and Sauvageau, 2003; Park et al., 2003). Interestingly, the multipotent state of emigrating neural crest cells has been likened to that of hematopoietic stem cells, and these cell populations share some commonality of gene expression, suggesting some similarities in developmental mechanisms (Orkin and Zon, 1997; LaBonne and Bronner-Fraser, 1999).

We speculate that while the PcG genes likely play a role in development of a diverse set of cell types and tissues, the relatively specific expression domains of some complex members imply that they may be involved in development of specific cell types, or may function to recruit other, more ubiquitously present PcG proteins to specific cell populations. Indeed, it has been suggested that the composition of Polycomb complexes may differ depending on cell type or developmental process (Otte and Kwaks, 2003; Sparmann and van Lohuizen, 2006; Squazzo et al., 2006). Therefore, based on our expression analysis, we propose that Bmi-1 may participate specifically, but not uniquely, in the development of neural plate border cells which include neural, neural crest, and placode progenitors. Since Bmi-1 is continuously expressed by progenitors of this region until their terminal differentiation, this stem cell factor probably

functions in multiple stages and aspects of neural crest development that involve maintenance of multipotency.

In an attempt to gain insight into the functionality of Bmi-1 in neural crest development, we performed *in vivo* loss-of-function experiments by antisense morpholino (MO) electroporation. When Bmi-1 MO is electroporated at gastrula stage into the prospective neural plate, expression levels of *Msx1*, as assayed by QPCR and *in situ* hybridization, are increased by early neurula stages. By whole-mount *in situ* hybridization, we find that the severity of the phenotype varies, likely due to an inability to control precise localization and amount of injected material, as well as due to weak penetrance of morpholino in this type of experiment in general (Mende et al., 2008). In addition, it is unlikely that a strong phenotype would be elicited by reduction of a single PcG member, as evidenced by the fact that some transgenic mouse lines carrying null mutations in single PcG genes do not exhibit severe defects or embryonic lethality (Chamberlain et al., 2008; Pietersen and van Lohuizen, 2008). Accordingly, we do not see a phenotype as a result of Bmi-1 over-expression alone, and only a weak repression of *Msx1* when Ring1B is additionally co-electroporated. However, given the limitations of the system, we are encouraged by the fact that we are able to see reproducible and statistically significant phenotypes as a result of Bmi-1 knock-down and over-expression.

The Bmi-1 MO phenotype is mainly manifested within the normal expression domain of *Msx1*, which indicates that Bmi-1 regulates this factor specifically in the neural plate border cell population. No mediolateral shift in the position of the neural plate border was observed in our Bmi-1 MO or over-expression experiments, suggesting that cross-repressive interactions between

juxtaposed neural and non-neural tissues are not affected, despite widespread distribution of electroporated material (McLarren et al., 2003; Woda et al., 2003). Rather, there was an observable increase or decrease in staining intensity within the neural plate border, which contains a heterogeneous population of cells marked by “salt-and-pepper” expression of specifier genes, which we are not yet able to resolve on a single cell level. Therefore, it is possible that by knocking down *Bmi-1* in this region, we are inducing *Msx1* in neural plate border cells that may not express it otherwise, and conversely, forced *Bmi-1* over-expression may extinguish *Msx1* transcripts in some of these progenitors. Alternatively, *Bmi-1* may function to maintain a threshold level of *Msx1* transcripts in neural plate border cells that is necessary for finely tuned control of downstream neural crest specifiers, but we are unable to distinguish between these possibilities at the present time.

It is likely that the phenotype elicited by *Bmi-1* MO is due to a direct effect on transcription and is not secondary to changes in the cell proliferation. Although we detected a slight increase in cell proliferation in ectodermal and neural tissues that have been electroporated with *Bmi-1* MO, dorsal neural fold progenitors were not affected. We found the proliferation increase surprising in light of mouse stem cell studies that have demonstrated a positive effect of *Bmi-1* on the cell cycle (Molofsky et al., 2003; Park et al., 2003). It is possible that the phenotype we observe is a secondary consequence of an upstream effect of *Bmi-1* MO on ectoderm- or neural-specific survival factors. In addition, the *Ink4a/Arf* locus through which *Bmi-1* functions to regulate proliferation in the mouse embryo is not conserved in the chicken genome. Thus, the role of *Bmi-1* in cell

cycle regulation may differ between the two species (Jacobs et al., 1999a; Kim et al., 2003).

We asked whether Bmi-1 regulates neural crest specifier genes in a similar manner to *Msx1* by assaying MO-electroporated embryos by *in situ* hybridization for expression of *FoxD3*, *Snail2*, and *Sox10* at HH8-10, stages during which these genes are highly expressed by pre-migratory and emigrating neural crest cells. Because the results were inconsistent, we suspect that these effects may occur as a secondary consequence of the Bmi-1 MO effect on upstream regulators and other neural crest specifier genes (Meulemans and Bronner-Fraser, 2004). Erratic changes in *Snail2* expression with Bmi-1 MO may also be due to perturbation of a feedback loop between the two factors, while *FoxD3* may be indirectly affected by an upregulation of an unknown repressor (Bermejo-Rodriguez et al., 2006). Therefore, by the time that we assay Bmi-1 MO embryos for changes in neural crest specifier expression by *in situ* hybridization, the results may already be confounded by perturbation of other, upstream regulatory interactions. In addition, the neural crest population is highly plastic and self-regulatory, which enables it to compensate for early effects of perturbations, especially if the phenotype is already weak. This has presented a challenge in our MO and over-expression experiments and we have been unable to determine whether neural crest migration or differentiation is altered by the electroporation because the phenotype appears normal when we culture embryos to the stages at which these processes may be examined.

In light of these limitations we decided to analyze Bmi-1 MO-electroporated embryos for changes in neural crest specifier expression by QPCR at HH6, when some of these factors first appear in the neural folds at low levels

(near or just below the threshold for detection by *in situ* hybridization), and when compensation for the MO effect may not yet have occurred. The results demonstrate a quantifiable increase of *FoxD3* and *Sox9* transcripts with Bmi-1 MO at HH6, suggesting that Bmi-1 is functioning to negatively regulate neural crest specifiers during early development. We hypothesize that this may serve to prevent their premature activation or upregulation in the neural folds, possibly in order to prevent premature commitment to the neural crest lineage. For example, although *FoxD3* is expressed in the neural plate border at HH4, it does not begin to accumulate in the dorsal neural folds until HH6-7 (Fig. 2.1, Chapter 2), and Bmi-1 may be preventing premature recruitment of *FoxD3* to dorsal neural tube progenitors. In turn, *Sox9* is not expressed in the chick embryo prior to HH6 (data not shown), and it is possible that PRC1-mediated repression is one of the mechanisms that prevent premature activation of late neural crest specifiers. Interestingly, some of the upstream factors that induce neural crest specifiers, such as *Msx1*, are present continuously during early development and may need to be modulated in some way that prevents continuous activation of target genes. This modulation may involve PcG repression at early stages in order to maintain *Msx1* levels below the threshold necessary for neural crest specifier induction or upregulation. In this case, the early increase in *FoxD3* and *Sox9* transcripts observed with MO may be a secondary consequence of an increase in *Msx1* levels due to Bmi-1 knock-down. Alternatively, these genes could be regulated independently. In conclusion, these data represent the first step in elucidating the role of Bmi-1 in neural crest development *in vivo*, which we demonstrate to involve early-acting negative regulation of neural plate border and neural crest specifier genes in the neural plate border region.

ACKNOWLEDGEMENTS

I am grateful to my co-advisor, Tatjana Sauka-Spengler, for providing sound collaboration, constructive discussion, and technical assistance and advice. I would also like to thank Matt Jones and Mary Flowers for their assistance. I am grateful to Kyoichi Isono for the generous gift of monoclonal Ring1B antibody. I would also like to thank Sujata Bhattacharyya, Meyer Barembaum, Jack Sechrist, and Sonja McKeown for helpful discussion and advice. This work was supported in part by the Ira Simon Fellowship.

Figure 3.1: *Bmi-1* is expressed during gastrulation in the chick embryo

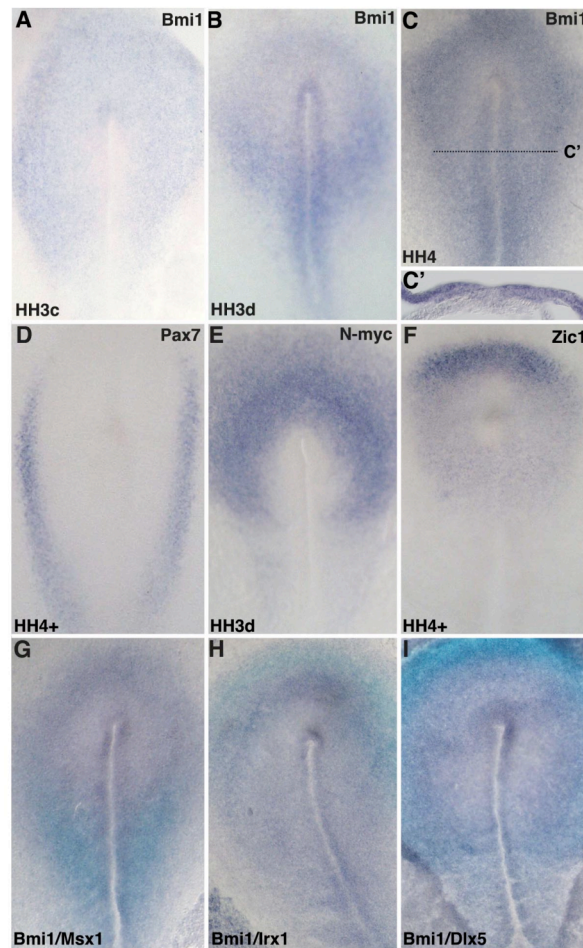


Figure 3.1. Chick *Bmi-1* is expressed in neural crest progenitors during gastrulation. **A.** At HH3c, *Bmi-1* is expressed at low levels throughout the epiblast. **B.** *Bmi-1* becomes restricted to the prospective posterior neural plate border at HH3d. **C** and **C'.** *Bmi-1* transcripts mark the prospective neural plate border both anteriorly and posteriorly at HH4. **D.** The expression pattern of *Bmi-1* resembles that of *Pax7* during HH4+. **E.** *N-myc* expression in the neural plate border is similar to *Bmi-1*. **F.** Anterior expression of *Bmi-1* is similar to *Zic1*. **G.** *Bmi-1* (purple) is co-expressed in the posterior border with *Msx1* (blue). **H.** *Bmi-1*

(purple) shares part of its anterior expression domain with placodal specifier *Irx1* (blue). I. *Bmi-1* (purple) expression is complementary to ectodermal specifier *Dlx5* (blue).

Figure 3.2: *Bmi-1* is expressed throughout development prior to differentiation

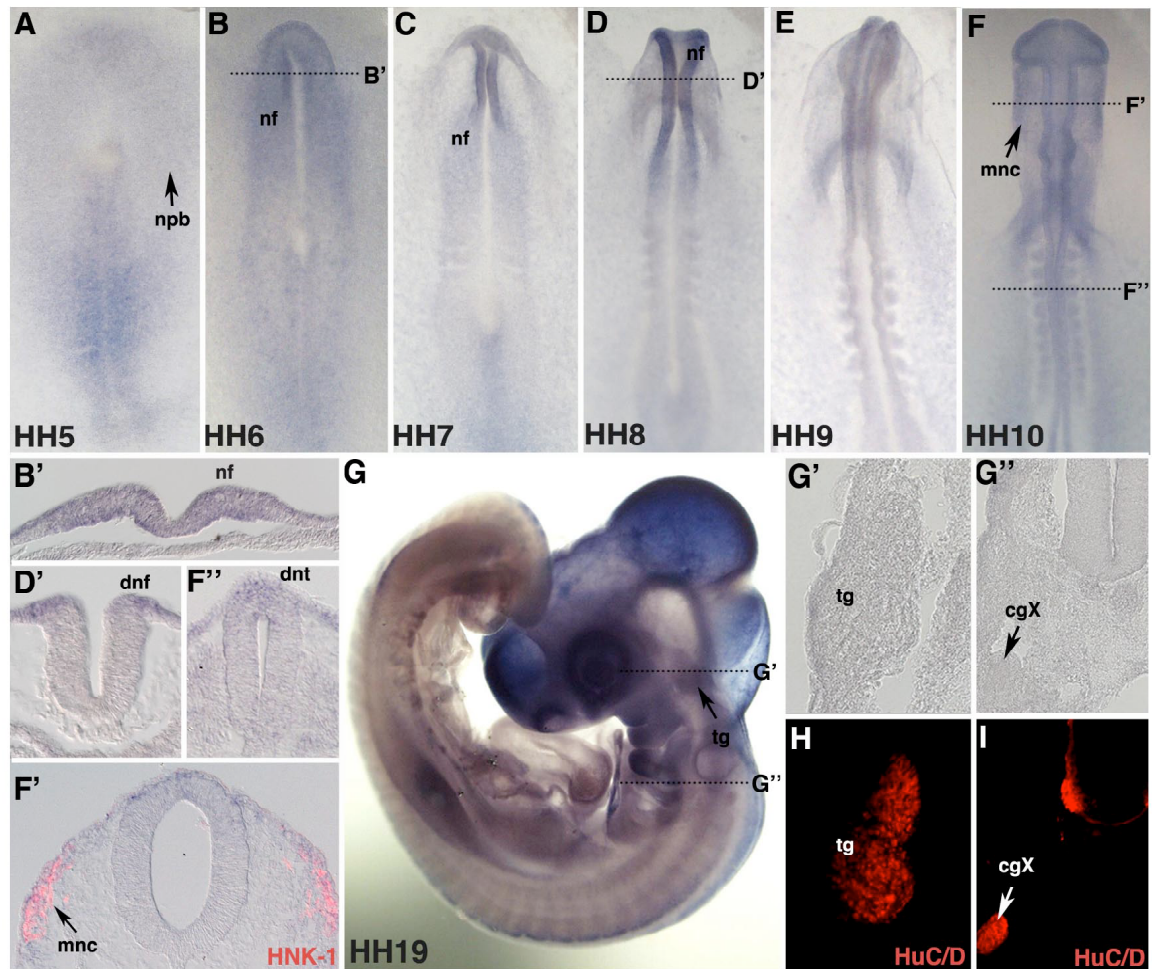


Figure 3.2. *Bmi-1* is expressed in neural crest progenitors during neurulation and early migration stages, but is downregulated in differentiated neural crest derivatives. **A.** At HH5, *Bmi-1* transcripts are localized in the neural plate border and primitive streak. **B** and **C.** At HH6 (**B**) and HH7 (**C**), *Bmi-1* is expressed in the neural folds and their border. **D.** At HH8, strong *Bmi-1* expression is observed in the dorsal aspect (**D'**) of the anterior neural folds. **E.** *Bmi-1* transcripts are maintained in neural tissue at HH9. **F.** At HH10, *Bmi-1* is expressed in migrating cranial neural crest cells that can be identified by HNK-1

immunostaining (**F'**), as well as in the dorsal neural tube at both cranial (**F'**) and trunk levels (**F''**). **G.** By HH19, *Bmi-1* transcripts are absent from the trigeminal (**G'**) and tenth cranial (**G''**) ganglia that express neuronal marker HuC/D (**H** and **I**, respectively). CgX, tenth cranial ganglion; dnf, dorsal neural fold; dnt, dorsal neural tube; mnc, migrating neural crest; nf, neural fold; npb, prospective neural plate border; tg, trigeminal ganglion.

Figure 3.3: Bmi-1 protein is actively translated during early development

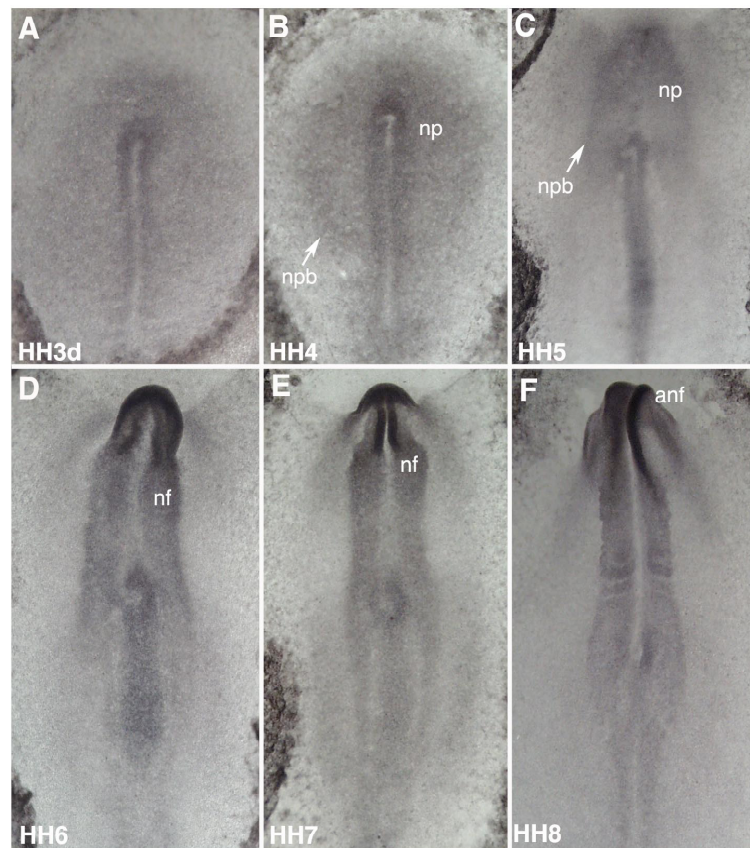


Figure 3.3. Bmi-1 protein expression recapitulates that of the mRNA during early developmental stages. Embryos were immunostained with a polyclonal Bmi-1 antibody and visualized with DAB enhanced with NiCo. **A.** Bmi-1 protein can be detected in the epiblast as early as HH3. **B.** Bmi-1 protein accumulates in the presumptive neural plate border (arrow) at HH4. It is also evident in the prospective neural plate. **C.** At HH5, Bmi-1 is expressed in forming neural tissue and neural plate border (arrow). **D** and **E.** Bmi-1 protein accumulates in the neural folds at high levels at HH6 and HH7. **F.** At HH8, Bmi-1 protein expression is highest in the anterior neural folds. Nf, anterior neural fold; nf, neural fold; np, neural plate; npb, prospective neural plate border.

Figure 3.4: PRC1 and PRC2 genes are expressed in the chick embryo

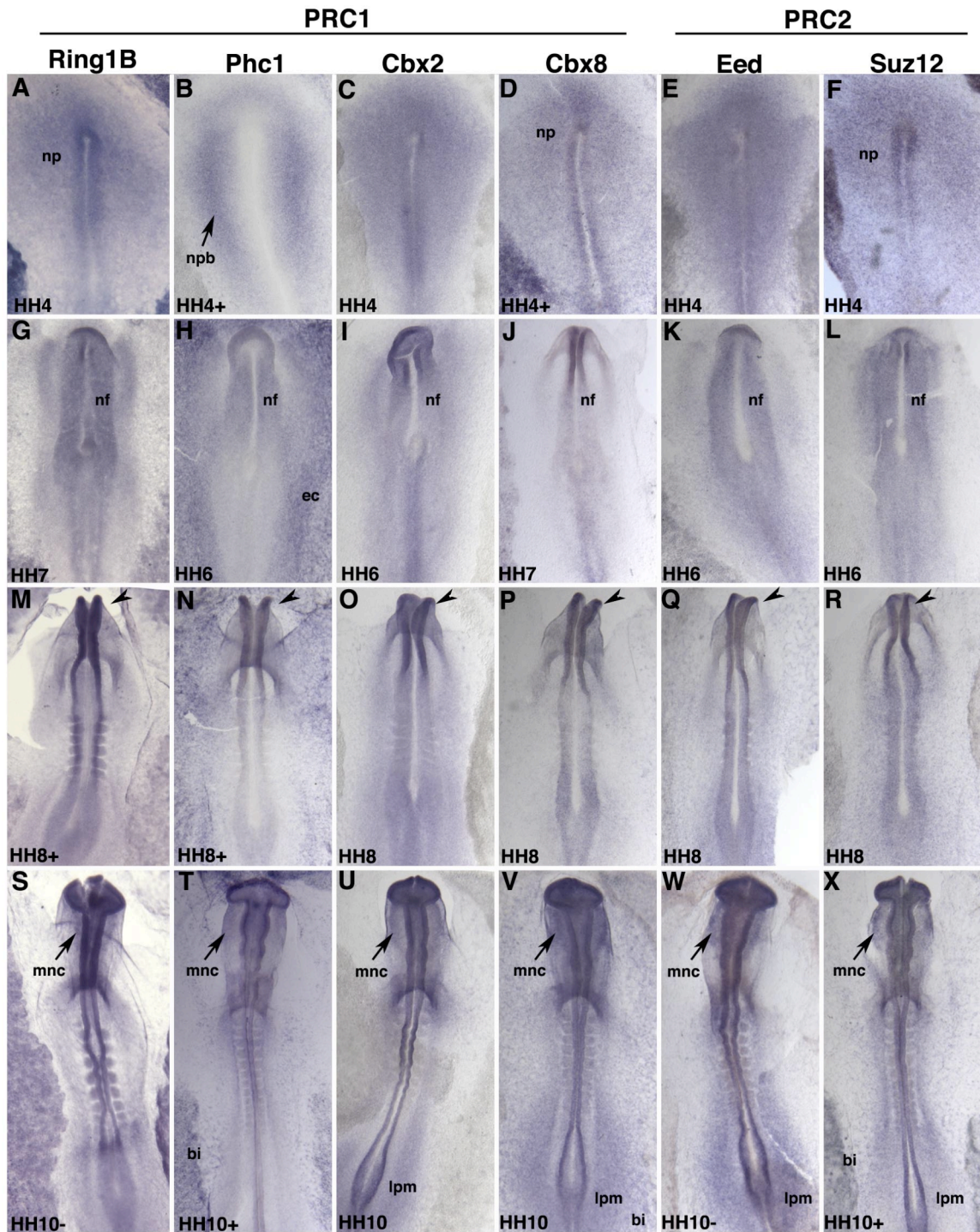


Figure 3.4. Four PRC1 genes and two PRC2 genes are expressed in overlapping but not identical domains during early stages of chick development. Embryos staged at approximately HH4 (**A-F**), HH6 (**G-L**), HH8 (**M-R**), and HH10 (**S-X**) were analyzed by whole-mount *in situ* hybridization using digoxigenin-labeled RNA probes for *Ring1B* (**A, G, M, S**), *Phc1* (**B, H, N, T**), *Cbx2* (**C, I, O, U**), *Cbx8* (**D, J, O, V**), *Eed* (**E, K, Q, W**), and *Suz12* (**F, L, R, X**). Expression in the anterior-most neural folds at HH8 and in migrating neural crest at HH10 is demarcated by arrowheads and arrows, respectively. Ao, area opaca; bi, blood islands; ec, ectoderm; lpm, lateral plate mesoderm; mnc, migrating neural crest; nf, neural fold; np, neural plate; npb, prospective neural plate border.

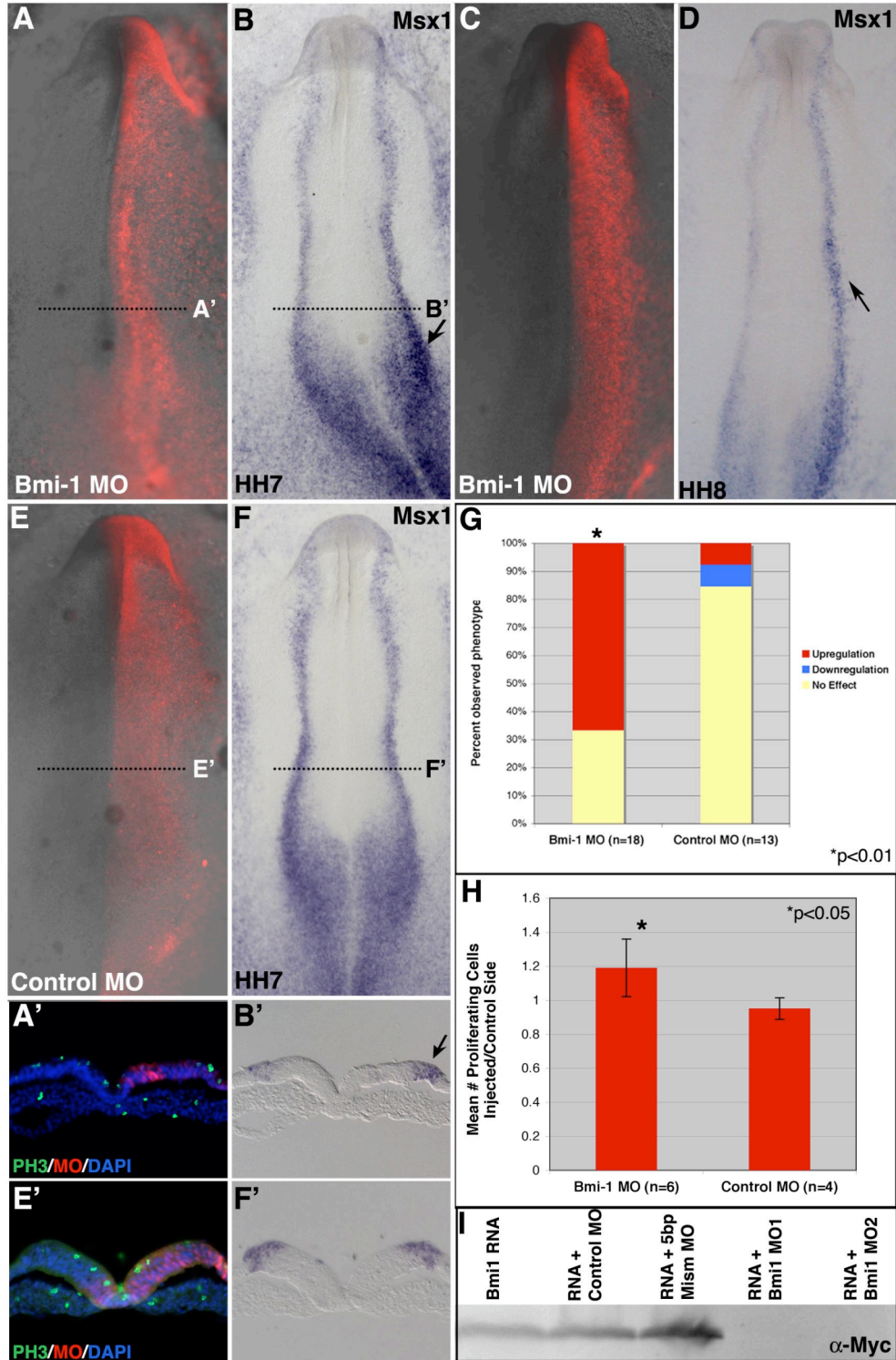
Figure 3.5: Effect of Bmi-1 knock-down on *Msx1* expression

Figure 3.5. Bmi-1 MO knock-down causes upregulation of *Msx1* expression. **A** and **A'**. Embryo that was electroporated with Bmi-1 MO at HH4 showing distribution of the MO at HH7. **B** and **B'**. *Msx1* is upregulated (arrow) on the electroporated side of the embryo shown in **A**. **C** and **D**. Bmi-1 MO-electroporated embryo (**C**) collected at HH8 shows a weaker upregulation of *Msx1* (**D**). **E**, **F**, **F'**. Control MO electroporation (**E**) does not affect *Msx1* expression (**F,F'**). **G**. Quantification of embryos exhibiting specific phenotypes shows that the effect observed with Bmi-1 MO is statistically significant. **H**. Graph illustrating mean number of phospho-histone H3-positive cells on the electroporated versus control side in sections of embryos injected with Bmi-1 MO (**A'**) or control MO (**E'**). **I**. MO specificity test shows that two different Bmi-1 MOs inhibit translation of *Bmi-1* mRNA when co-injected into *Xenopus* embryos, while control MOs do not.

Figure 3.6: Quantification of changes in gene expression due to Bmi-1 MO

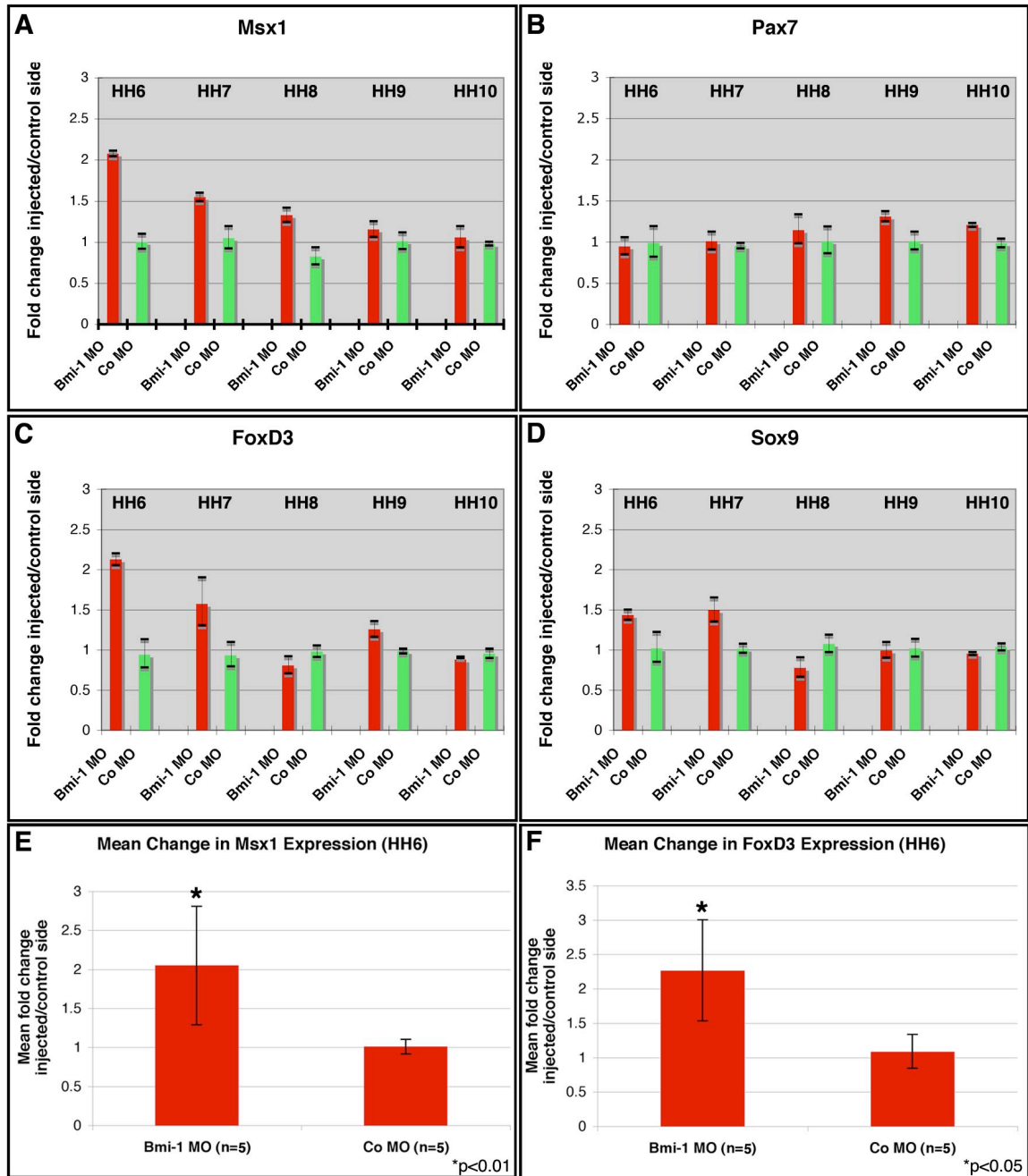


Figure 3.6. Fold change in transcript expression levels as a result of Bmi-1 MO knock-down was measured by QPCR. Embryos were electroporated at HH4 with either Bmi-1 MO or control MO and cultured until HH6-10. Electroporated

embryos collected at specific stages were laterally bisected to separate the electroporated and control sides and RT-QPCR was performed to compare changes in expression levels of target genes between the two halves within the same embryo. **A-D**. Fold change in expression levels of *Msx1* (**A**), *Pax7* (**B**), *FoxD3* (**C**), and *Sox9* (**D**) with Bmi-1 MO or control MO in single representative embryos collected at each stage indicated. **E** and **F**. Mean change in transcript levels of *Msx1* (**E**) and *FoxD3* (**F**) in 5 embryos that were electroporated with Bmi-1 or control MO and analyzed at HH6.

Figure 3.7: Bmi-1 and Ring1B co-over-expression causes *Msx1* downregulation

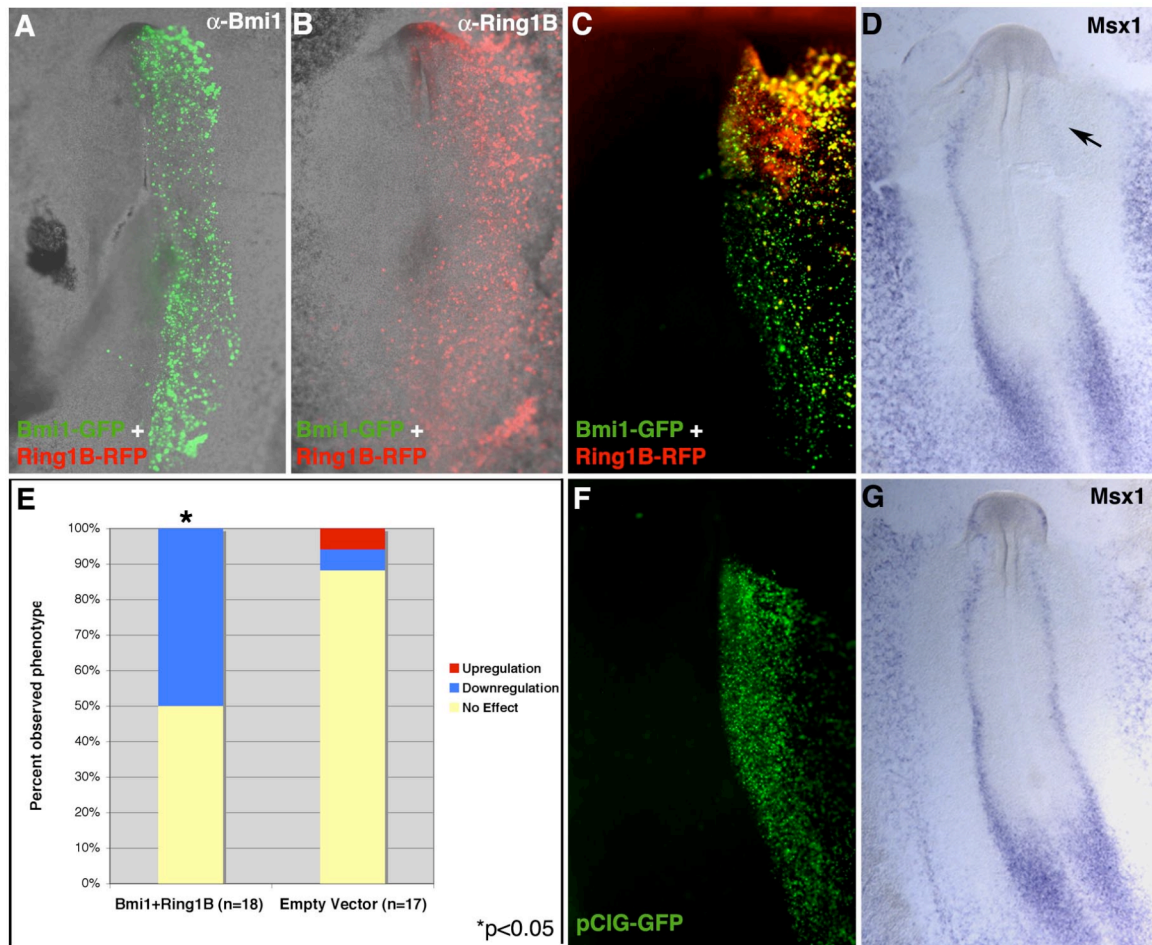


Figure 3.7. Co-over-expression of Bmi-1 and Ring1B in the chick gastrula results in a downregulation of *Msx1* transcripts at neurula stage. pCIG-Bmi-1-GFP and pCIG-Ring1B-memRFP constructs were co-electroporated at HH4 targeting the prospective neural plate border region. **A.** An electroporated embryo immunostained with anti-Bmi-1 antibody showing that large amounts of protein are translated on the injected side at HH6. **B.** Excess Ring1B protein can also be detected as early as HH6 in an embryo co-electroporated with Bmi-1 and Ring1B. **C and D.** An embryo that has been electroporated with pCIG-Bmi-1-GFP and

pCIG-Ring1B-memRFP shows distinct downregulation of *Msx1* transcripts on the electroporated side. **F** and **G**. Empty pCIG-GFP vector control electroporation (**F**) does not cause a significant change in *Msx1* expression (**G**). **E**. Downregulation of *Msx1* is observed in 50% of embryos co-electroporated with Bmi-1 and Ring1B (9/18, $p < 0.05$). In contrast, 74% of embryos electroporated with pCIG-GFP empty vector do not exhibit a phenotype (14/19).